Carbon Resources Conversion 2 (2019) 43–50

Contents lists available at ScienceDirect

Carbon Resources Conversion

journal homepage: http://www.keaipublishing.com/en/journals/carbon-resources-conversion

Continuous monitoring of char surface activity toward benzene

Cheolyong Choi[a], Kentaro Shima[b], Shinji Kudo[b], Koyo Norinaga[c], Xiangpeng Gao[d], Jun-ichiro Hayashi[b,e,*]

[a] Interdisciplinary Graduate School of Engineering Sciences, Kyushu University, 6-1, Kasuga Koen, Kasuga 816-8580, Japan
[b] Institute for Materials and Engineering Chemistry, Kyushu University, 6-1, Kasuga Koen, Kasuga 816-8580, Japan
[c] Department of Materials Science and Engineering, School of Engineering, Nagoya University, Nagoya 464-8601, Japan
[d] Discipline of Electrical Engineering, Energy and Physics, School of Engineering and Information Technology, Murdoch University, 90 South Street, Murdoch, WA 6150, Australia
[e] Transdisciplinary Research and Education Center of Green Technology, Kyushu University, 6-1, Kasuga Koen, Kasuga 816-8580, Japan

HIGHLIGHTS

- A continuous measurement method for char activity toward benzene was developed.
- Benzene vapor was decomposed over a micro fixed bed of char under pyrolytic condition.
- The presence of consumptive Type I and non-consumptive Type II surfaces was observed.
- Type II surface converted benzene into diaromatics and carbon deposit.

ARTICLE INFO

Keywords:
Carbon deposition
Aromatics
Tar
Char
Kinetics
Pyrolysis
Gasification

ABSTRACT

Kinetics of thermal decomposition of benzene on lignite-derived char was investigated at 900 °C by applying a new method to continuously monitor the char surface activity. Benzene vapor was continuously forced to pass through a micro fixed bed of char with residence time as short as 7.6 ms, and then detected continuously by a flame-ionization detector. Results showed the presence of two different types of char surfaces; consumptive Type I surface and non-consumptive (sustainable) Type II surface. Type I surface of a partially CO_2-gasified char had an capacity of carbon deposit from benzene over 20 wt%-char and an initial activity (represented by a first-order rate constant) as high as 160 s^{-1}. Both of them decreased with increasing carbon deposit due to consumption of micropores accessible to benzene, and finally became zero leaving Type II surface that had a very stable activity with rate constant of 4 s^{-1}. The chars without gasification had capacities of Type I surfaces smaller by two orders of magnitude than the partially gasified char, while the Type II surfaces had activities similar to that of the partially gasified char. It was found that Type II surface converted benzene into not only carbon deposit but also diaromatics and even greater aromatics. Composition of the greater aromatics was unknown because they were deposited onto the reactor wall immediately after passing through the char bed.

1. Introduction

Elimination of tar (i.e., aromatic compounds) has been an important technical issue of gasification of coal and biomass operated at temperature lower than 1000 °C. It is recognized that use of char is a most effective way to eliminate the tar, as reviewed by Devi et al. [1], Abu El-Rub et al. [2], Li [3] and Hayashi et al. [4]. Ability of char to enhance the tar decomposition was first reported by Chembukulam et al. [5], who showed near complete decomposition of tar from the pyrolysis of woody biomass within a charcoal bed at 950 °C. Such effectiveness of using charcoal was demonstrated for continuous gasification of woody biomass by Brandt et al. [6]. Extensive decomposition of tar was also reported by Hayashi et al. [7] and Iwatsuki et al. [8], who performed lignite pyrolysis in drop-tube reactors with continuous co-feeding of steam and the pulverized lignite, and found simultaneous and rapid progress of steam gasification of nascent char and decomposition of nascent tar over the char at temperature of 800–900 °C. Then, many researchers reported reduction of tar concentration in the product gas by employing char from coal or biomass with varieties of reactors, atmospheres, temperatures and fuel types [9–27].

* Corresponding author at: Institute for Materials and Engineering Chemistry, Kyushu University, 6-1, Kasuga Koen, Kasuga 816-8580, Japan.
E-mail address: Junichiro_hayashi@cm.kyushu-u.ac.jp (J.-i. Hayashi).

https://doi.org/10.1016/j.crcon.2018.12.001
Received 8 October 2018; Received in revised form 28 November 2018; Accepted 7 December 2018
Available online 13 December 2018

Mechanism and kinetics of tar decomposition on char surface have been studied [28–35]. Hosokai et al. [28] investigated decomposition of model compounds (mono- to tetra-aromatic hydrocarbons and phenol) over a wood char in the presence/absence of steam and H_2 in the atmosphere. Among the aromatics employed, benzene and naphthalene were the most and second most refractory. In the absence of steam, the char activity (represented by once-through conversion of aromatics) was lost by accumulation of deposited carbon in/on the porous system of the char, in other words, consumption of pores. They claimed that 'consumptive' micropores (size < 1.5 nm) were responsible for the activity while estimated that mesopores played a role of introducing vapor into micropores. They also found that the char activity was maintained if the steam gasification (micropore creation) occurred at a carbon-based rate equivalent with or greater than that of carbon deposition (micropore consumption).

Kinetics of decomposition of aromatic compounds over char was also investigated by other research groups [29–35]. A common conclusion from those studies was that the activation (gasification) of the char greatly enhances its activity making it more durable. The researchers also made a focal point on a particular behavior of the char, that is, deactivation due to loss of micropores [28,33] or mesopores [35]. Fuentes-Cano et al. [34] reported that the char activities toward naphthalene and toluene decreased with time in the absence of steam (i.e., under pyrolytic conditions) and also in its presence at concentration insufficiently high for fast char gasification *in-situ* recuperating it. The conversion of aromatics decreased to a level equivalent to that for a reference material (SiC), suggesting complete or near-complete deactivation of the char. Fuentes-Cano et al. [35] also performed decomposition of naphthalene over pre-activated chars under pyrolytic conditions, and found that the naphthalene conversion decreased and then became near stable within a certain range (20–60%). Similar trends were reported by Burhenne and Aicher [32] who showed time-dependent changes in the activities of pre-activated chars toward benzene. Nestler et al. [33] investigated the decomposition of naphthalene over non-activated chars and activated ones. They reported that the activity of a non-activated char was lost quickly and completely or near completely at 850 °C while another char lost its activity more slowly and not completely.

In view of the above, it is hypothesized that both pre-activated and non-activated chars lose its activity, unless the gasification occurs *in-situ* at a sufficient rate, but not completely, leaving a certain level of activity, in other words, the char has two different modes of activities. This was a motivation of this work. Another motivation was necessity of further improvement of the experimental system. The previous reactors and operating conditions were not necessarily optimized for monitoring the char activity that can greatly change over ranges from full conversion of aromatics to near zero. Those reactors were not necessarily 'differential' reactors, rather, 'integral' ones with gas residence times of 50–200 ms (except some examples [32]). Such residence time could be too long to derive kinetics of aromatics decomposition correctly. Such long residence time could also vary the composition of gaseous species and the activity of char along the bed axis. Intermittent measurement of conversion of aromatics with long intervals could miss quick change in the char activity, in particular, very early and quick deactivation.

This work primarily aimed to continuously measure the char activity for benzene decomposition under pyrolytic condition over the entire range up to complete loss of the activity as a function of amount of carbon deposit as well as time, expecting critical examination of the above-described hypothesis. For accomplishing this purpose, the authors developed a new measurement system that consisted of a micro fixed bed of char, a flame ionization detector, as well as benzene vapor generator and distribution lines. Continuous measurements were combined with intermittent and batch analyses of light gases, benzene (feed) and lighter/heavier products.

2. Experimental

2.1. Material

Three different chars were prepared and used. The lignite sample was prepared from a Victorian lignite, Loy Yang, which was dried partially leaving some moisture (ca. 10 wt%) and pulverized to sizes smaller than 106 μm prior to use. A char sample (Char-1) was prepared by pyrolyzing the lignite in atmospheric flow of N_2 with heating rate and peak temperature of 10 °C/min and 900 °C, respectively. The contents of metallic species of Char-1 were as follows: Na; 0.15, K; 0.009, Mg; 0.13, Ca; 0.097 wt%-char. The lignite sample was also subjected to sequential acid treatments in aqueous solutions of HCl (3 mol/L), HF (3 mol/L) and then HCl (3 mol/L) for removal of major metallic species (Na, Ca, Mg, and Fe), Si- and Al-containing species. The acid-washed lignite, of which the contents of Na, K, Mg, and Ca were respectively 0.00027, 0.00026, 0.00048, and 0.0018 wt%-coal, was pyrolyzed under the same conditions as above. The resulting char is hereafter referred to as Char-2. This char was gasified with CO_2 up to a mass-based conversion of 60%. Temperature and atmosphere were 900 °C and an equimolar CO_2/N_2 mixture, respectively. The partially gasified Char-2 is termed Char-3. All of the char samples were sieved to collect fraction with particle sizes of 38–75 μm, and then used for experiments. The char samples were subjected to N_2 adsorption/desorption at −196 °C with an analyzer (Quantachrome Instruments, model Autosorb®-iQ). Table 1 shows properties of the char samples relevant to their porous natures. Benzene of a guaranteed reagent grade (Wako Chemicals Co., Japan) was chosen as a model compound of tar, and used without further purification.

2.2. Continuous monitoring of benzene decomposition over char

Fig. 1 shows a schematic diagram of the apparatus. It consists of three main components (vaporizer, reactor and flame ionization detector (FID)) and controllers and parts. An asymmetrical U-shaped tube is used as the vertical reactor. It is made of transparent quartz glass with inner diameters of 6.0 and 4.0 mm at the inlet and outlet sides, respectively. A photograph of the U-tube is available in Supplementary Information. The reactor is packed with a bed of char particles (mass of char; 20 mg, bed height; 1.8 mm, bulk density; 0.40 g/cm^3), which is fixed at near-bottom of the upstream part.

The benzene vaporizer consists of a cylindrical glass bottle with a volume of 50 ml. The primary carrier gas (N_2, purity > 99.9996 vol%) is continuously introduced into the headspace of the bottle at a rate of 20 ml/min (at 1.0 atm and 25 °C), where benzene is vaporized at a

Table 1
Porous nature of fresh char. Before exposed to benzene vapor.

Sample	Specific surface area (BET), m^2/g	Specific surface area (QS-DFT[a]), m^2/g	Pore volume (QS-DFT), cm^3/g	Average pore width[b] (QS-DFT), nm
Char-1	205	190	0.15	0.8
Char-2	220	185	0.13	1.4
Char-3	1890	1730	0.75	1.3

[a] Quenched solid density functional theory. Slit pores were assumed.
[b] Slit pores were assumed.

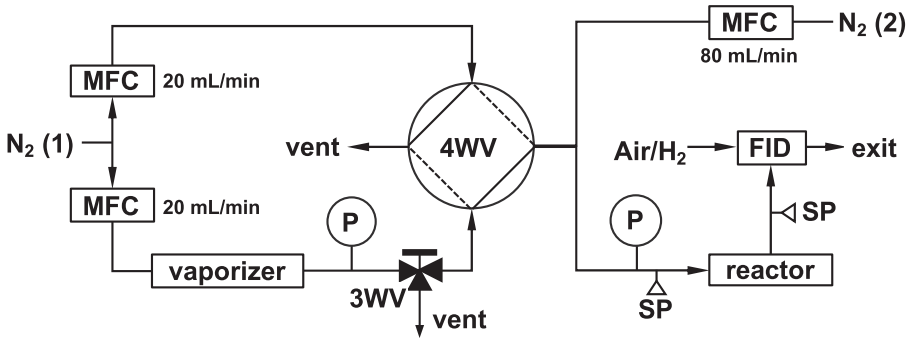

Fig. 1. Schematic diagram of experimental system. 3WV and 4WV; 3-way and 4-way valves, respectively, FID; flame ionization detector (originally installed in a gas chromatograph, Shimadzu Co. Ltd, model GC-14B), MFC; mass flow controller, N_2 (1) and N_2 (2); primary and secondary carrier gases, respectively, P; pressure monitor, SP; gas/vapor sampling port.

steady rate. The benzene vapor is diluted by the secondary N_2 (80 ml/min) to a concentration within a range of approximately 1100–1600 ppmv (3.8–5.6 g-benzene/Nm^3), and then fed into the reactor for a prescribed period of time (30–120 min). The benzene concentration is controlled by varying the temperature of the vaporizer. The gas residence time within the char bed is calculated as 7.6 ms on an empty basis at 900 °C. The near-entire portion of the exit gas (except a very small portion for intermittent sampling) is introduced continuously into the FID that detects benzene (unconverted) and the other hydrocarbon species, if any, together. The FID response is monitored and recorded continuously. During the feeding of benzene vapor into the reactor, small portions of gas (0.4-ml for each) are sampled at the reactor upstream and downstream intermittently and analyzed with a gas chromatograph (Shimadzu, model GC-14B) that is equipped with an FID and columns for gas separation and CO/CO_2 methanation. The conversion on benzene was determined directly by its concentrations upstream/downstream the reactor. This made possible to quantify the downstream concentration continuously from the FID response.

Table 2 lists the conditions for the individual blank tests without char bed (B) and runs with char bed (R). Three runs, B1.3, R2.5 and R4.4, were performed exclusively for collecting the condensable organic matter (benzene and heavier aromatics) completely at the reactor downstream, and analyzing the composition by gas-chromatography mass spectrometry (GC/MS) on a Perkin Elmer model, Clarus SQ8.

Fig. 2(a) shows the FID responses during a sequence of blank tests, B1.1 and B1.2, without char bed. The horizontal axis indicates the time elapsed since the switching of the 4-way valve (see Fig. 1) to start supply of benzene vapor to the reactor. Each FID signal occurs around 0.1 min, which is time required for the gas to travel between the 4-way valve and the FID (see Fig. 1). Then, the intensity increases steeply and becomes steady within 0.8 min. The shapes of the curves are different from those for 'ideal' step responses, and this is believed to be due to unavoidable back mixing of the gas. It is more importantly noted that the signal profiles in the two tests are highly reproducible. Each signal is arisen from not only benzene but also other hydrocarbons if formed in the reactor. It was confirmed in a test (B1.3) that benzene conversion in the gas phase was steady at 0.45% on carbon basis giving two aromatic compounds (biphenyl; 0.43%, naphthalene 0.02%) while neither light hydrocarbons such as CH_4 nor soot was detected. Fig. 2(b) shows the results from a sequence of R1.1 and R1.2 with high reproducibility of the FID response. Benzene was not decomposed at all even at 700 °C in the presence of Char-1. It was thus confirmed that the FID response was reproducible unless benzene underwent decomposition over the char.

3. Results and discussion

3.1. Decomposition of benzene on Char-3

Fig. 3 shows the FID responses in a sequence of two runs with Char-3, i.e., R4.1 and R4.2. In the former run, the FID signal intensity increases gradually and becomes steady at 36 min. It is also seen that the signal intensity after 36 min is slightly but systematically lower than 100% that corresponds to no benzene conversion. In R4.2 with the spent Char-3 from R4.1, the signal intensity is steady over the period of benzene feeding and at the same level as that at 36–50 min in R4.1. Though not shown, the signal intensity at 97% was maintained in the following run (R4.3, 80 min). This result indicates that Char-3 had two different types of surfaces. One was *very active but consumptive*, and the other was *less active but non-consumptive*. These are hereafter referred to as *Type I* and *Type II surfaces*, respectively.

Fig. 4 exhibits the difference in the FID intensity between R4.1 and R4.2 as a function of time. The vertical axis means the benzene conversion into carbon (C) deposit on Type I surface. The initial conversion is around 70%, which corresponds to a first-order rate constant as high as 160 s^{-1}. The rate constant, k, is hereafter expressed by the first-order rate equation ($\frac{dX}{dt} = k(1 - X)$, where, X and t represent the benzene conversion into C deposit and the time exposed to benzene vapor, respectively). Within the interval of 0–36 min in R4.1, no carbon deposit was detected at either the upstream or downstream of the char bed, and it is therefore judged that the benzene conversion shown in Fig. 4 is equivalent to that into C deposit onto Type I surface of Char-3. In R4.4 with fresh Char-3 and benzene feeding time of 30 min, biphenyl and naphthalene were recovered at the reactor downstream. Their respective yields, 0.41% and 0.02%, were almost the same as those in B1.3 (0.43% and 0.02%, respectively). It was believed that these diaromatic compounds were formed in the gas phase at steady rates and probably at downstream of the Char-3 bed in R4.1–R4.3, contributing slightly to the FID signals shown in Fig. 3.

Further analysis of the results shown in Figs. 3 and 4 enables to determine the capacity of Type I surface of Char-3 for the C deposition from benzene. As seen in Fig. 5, Type I surface of Char-3 had a capacity as much as 22 wt% of its initial mass. On the other hand, the activity of Type II surface was much lower than that of Type I surface, but its activity was steady over the period of at least 140 min (R4.1–R4.3) with a rate constant of 4.0 s^{-1}. Although not demonstrated, it is estimated that the 'capacity' of Type II surface was *sustainable*. This feature is reasonably understood by considering autocatalytic nature of carbon deposition over carbon surface. Hosokai et al. investigated reforming of tar from the pyrolysis of woody biomass with mesoporous alumina. They reported that the alumina had a high ability to deposit vapor of aromatics onto its own acidic surface, and moreover, C deposit in mesopores further enhanced the carbon deposition increasing the tar removal [36]. Fuentes-Cano et al. reported that the activity of a type of char toward naphthalene decreased along with C deposition and then reached a certain level (well above zero) depending on the conditions [35]. Nestler et al. reported similar trends for decomposition of naphthalene [33]. The presence of Type I and Type II surfaces is thus consistent with those previous reports.

The specific surface areas (determined by applying QS-DFT) of the fresh Char-3, that after R4.4 (30 min exposure to benzene vapor) and spent Char-3 from R4.3 (cumulative exposure time = 140 min) were 1,730, 740 and 56 m^2/g, respectively. According to Fig. 4, Char-3 had lost 90% of the initial activity of Type I surface by 30-min exposure to

Table 2
Conditions of blank tests (B) and runs (R) with Char-1, Char-2 or Char-3.

ID	Temperature, °C	Bed material	Mass of bed material, mg	Benzene conc. ppmv	Gas flow rate @25 °C, cm^3/min	Feeding time, min	Remark
B1.1	900	none	–	1215	100	30	Benzene feeding was paused between runs, and resumed when FID response became stable.
B1.2		none	–			30	
B1.3	900	none	–	1140	100	80	Carried out exclusive for recovery/analysis of aromatic products.
R1.1	700	Char-1	20	1185	100	40	Sequential feeding of benzene to the identical bed of Char-1.
R1.2						40	Benzene feeding was paused between runs, and resumed when FID response became stable.
R2.1	900	Char-1	20	1245	100	30	Sequential feeding of benzene to the identical bed of Char-1.
R2.2				1245		30	Benzene feeding was paused among runs, and resumed when FID response became stable.
R2.3				1245		80	
R2.4				1290		120	
R2.5	900	spent Char-1 from R2.4	20[a]	1525	100	80	Carried out exclusively for recovery of benzene and heavier aromatics products.
R3.1	900	Char-2	20	1175	100	30	Sequential feeding of benzene to the identical bed of Char-2.
R3.2						30	Benzene feeding was paused among runs, and resumed when FID response became stable.
R3.3						80	
R4.1	900	Char-3	20	1275	100	50	Sequential feeding of benzene to the identical bed of Char-3.
R4.2						50	Benzene feeding was paused among runs, and resumed when FID response became stable.
R4.3						80	
R4.4	900	spent Char-3 from R4.3	20	1165	100	30	Carried out exclusively for recovery of benzene and heavier aromatics products.

[a] The entire portion of the spent Char-1 from R2.4 was used.

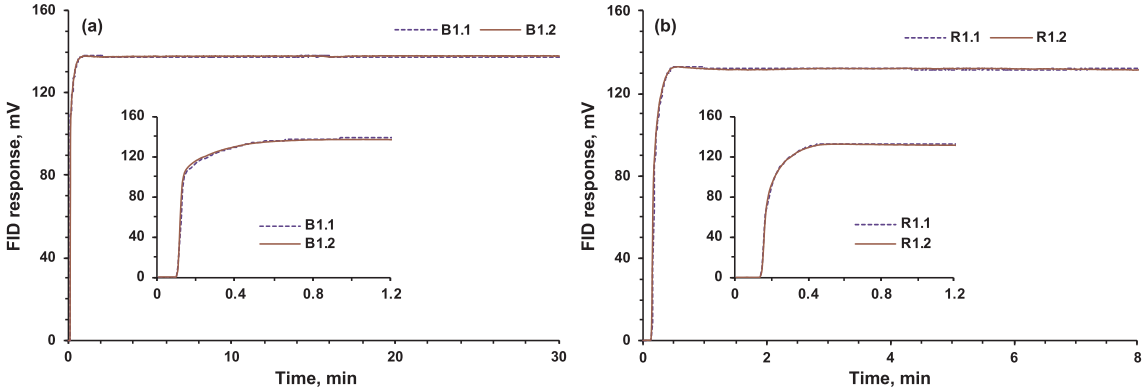

Fig. 2. FID signals recorded in B1.1–B1.2 (a) and R1.1–R1.2 (b). Conditions for the individual tests/runs are available in Table 2.

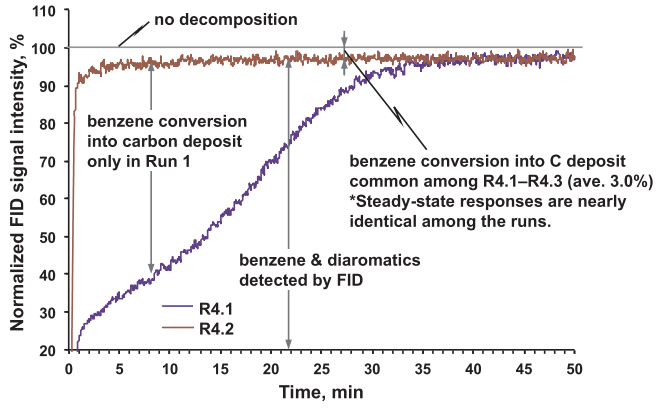

Fig. 3. FID responses in a sequence of two runs R4.1 and R4.2. The signal intensities are normalized by that with no benzene conversion.

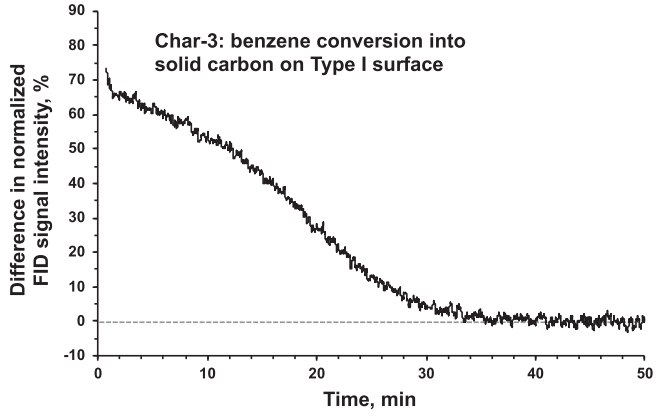

Fig. 4. Difference in the FID signal intensity between R4.1 and R4.2 corresponding to benzene conversion into carbon deposits on Type I surface of fresh Char-3 in R4.1.

benzene vapor (with respect to the benzene conversion), while the loss of the specific area was limited to 58%. Thus, the surface area arisen from micropores and mesopores was not a measure, or at least, not a direct measure for the Type I surface activity that greatly changed along with the C deposition. On the other hand, the activity of Type II surface seemed to be independent of the specific surface area, which decreased to *ca.* 1/30 of the initial until the end of R4.3. The characteristics of Type II surface is discussed in more detail in the following section.

3.2. Decomposition of benzene on Char-1 and Char-2

Fig. 6 shows the FID responses in the sequence of R2.1 and R2.2

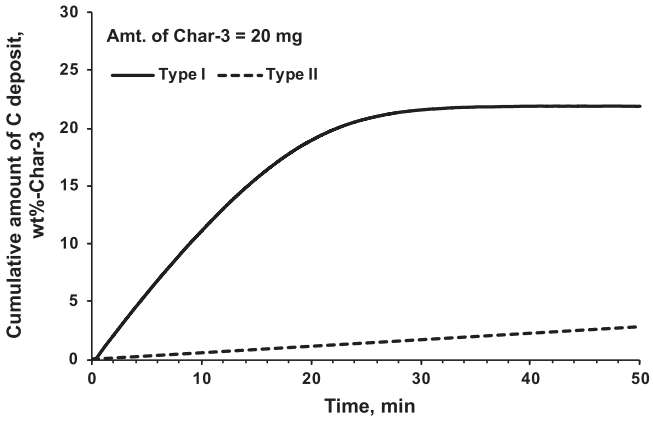

Fig. 5. Cumulative amounts of C deposits onto Type I and Type II surfaces in R4.1. The amount is normalized by the initial mass of Char-3. The amount of C deposit on Type II surface was calculated by assuming a steady conversion of benzene (3.0%) over the period of the sequential R4.1–R4.3.

with Char-1. There is difference in the signal intensity between these two runs, although it is much less significant if compared with that between R4.1 and R4.2. Char-1 had much smaller capacity of C deposit as well as much lower initial activity than Char-3. As shown in Fig. 7, the initial benzene conversion on Type I surface into C deposit is slightly over 10%. It is also seen that Type I surface loses the activity within 4 min. The capacity of the Type I surface was in fact as small as 0.18 wt% of the initial mass of Char-1, and it was only *ca.* 1/120 of the capacity of Char-3. On the other hand, the benzene conversion into C deposit on Type II surface was steady around 4.3% all through R2.1 to R2.4 (total period of benzene feeding; 260 min). Thus, Type II surface of Char-1 was slightly more active than that of Char-3. The specific QS-DFT surface areas of the fresh and spent Char-1 were 190 and 17 m^2/g, respectively. Taken together with the steady benzene conversion on Type II surface, it is suspected again that the activity of Type II surface is nearly independent of the micropore/mesopore surface area, at least for the reaction times examined. The above-mentioned steady benzene conversion on Type II surface (4.3%) corresponds to a first-order rate constant of 5.8 s^{-1}. This rate constant means benzene conversion of 0.44 if the residence time is 100 ms. Thus, the activity of Type II surface should not be ignored in a practical sense.

Two phenomena, which had not been reported so far, were found in R2.1 to R2.5. The first one was formation of biphenyl and naphthalene. Their yields were measured in R2.5, and determined as 1.1% and 0.04% on the carbon basis, respectively. These were small but systematically greater than those by the gas-phase reactions of benzene, i.e., 0.43% and 0.02%, respectively. This strongly suggests the formation of those diaromatics on Type II surface, because such diaromatics formation was not detected when Type I surface had sufficiently high activity, as will

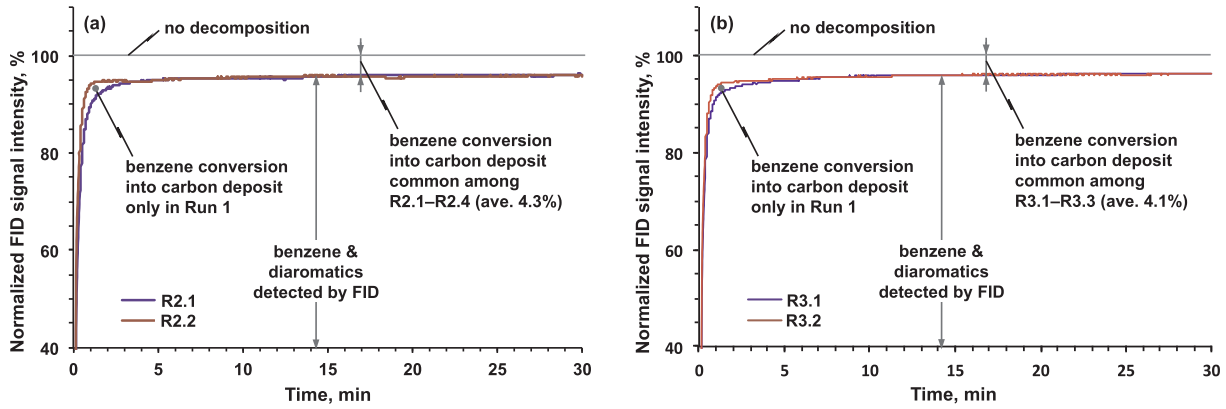

Fig. 6. (a) FID responses in a sequence of two runs R2.1 and R2.2. (b) FID responses in a sequence of two runs R3.1 and R3.2. The signal intensities are normalized by that for no benzene conversion.

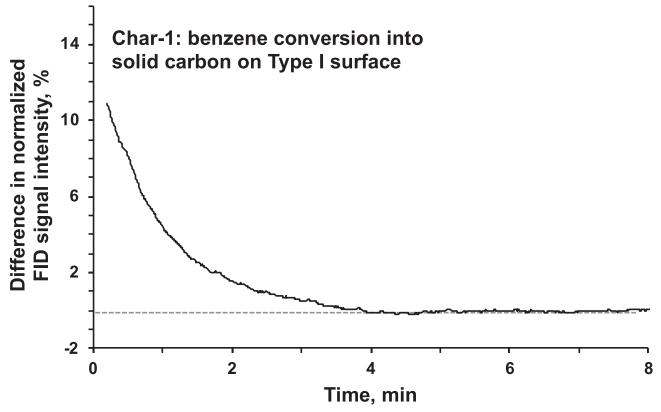

Fig. 7. Difference in the FID signal intensity between R2.1 and R2.2 corresponding to benzene conversion into carbon deposits on Type I surface of fresh Char-1 in R2.1.

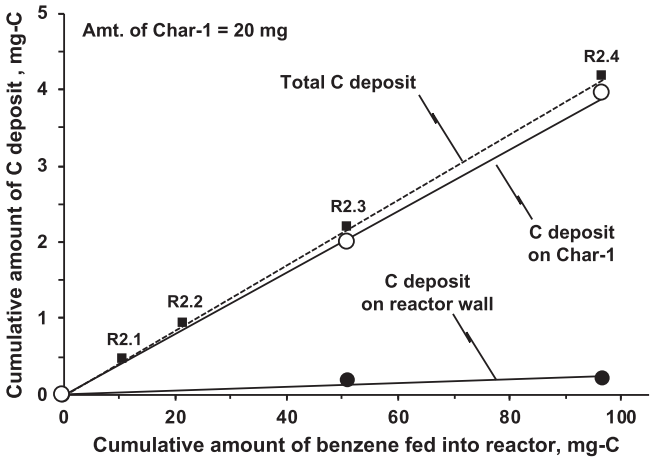

Fig. 8. Relationship between the cumulative amount of benzene fed into the reactor and that of C deposit. Total amount of C deposit (indicated by closed square) does not include that formed on Type I surface (0.036 mg-C, only in R2.1).

be mentioned later. It was also found that carbon deposition occurred onto the reactor wall at downstream of the char bed. It was believed that heavier aromatics were formed on Type II surface together with the diaromatics, desorbed from the surface, and then deposited onto the reactor wall. Such heavier aromatics, which was not identified by GC/MS at all, had a high propensity of conversion into C deposit, and therefore could not escape from the reactor.

Fig. 8 shows accumulation of C deposit on Type II surface of Char-1 and that on the reactor wall through R2.1–2.4. The linear increases in the amounts of C deposits demonstrate steady activity of Type II surface to form C deposit thereon, diaromatics, and heavier aromatics as the precursor of C deposit on the reactor wall. A photograph of the reactor after R2.2 is available in Supplementary Information. The above-described results indicate that benzene underwent not only conversion into C deposit but also aromatic ring condensation (and/or polymerization). It is suspected that the same or similar thermochemical events occurred in previous studies, but were missed probably due to the gas residence times within char bed were long enough to prevent heavier aromatics from escaping from the bed.

The activity of Char-2, which was prepared from the acid-washed lignite, was investigated by analyzing the results from R3.1–R3.3. The characteristics of Char-2 was not the same as but similar to those for Char-1, as shown in Table 3. Differences in the C deposit yields between Char-1 and Char-2 may be attributed to those in the porous properties and/or the presence of intrinsic metallic species, in particular, Na and Ca that have more or less catalytic activities toward aromatics if dispersed on carbonaceous surface [7,8,34].

Table 3
Comparison of properties of Char-1 and Char-2 relevant to activity for benzene decomposition.

Sample	Char-1	Char-2
Initial benzene conversion on Type I surface, % (first-order rate constant, s^{-1})	11 (15)	8.0 (11)
Capacity of Type I surface (amt. of C deposit), wt%-char	0.18	0.13
Steady-state benzene conversion to C deposit on Type II surface, % (first-order rate constant, s^{-1})	3.9 (5.3)	3.9 (5.4)
Steady-state benzene conversion to C deposit on reactor wall, %	0.38	0.07

3.3. Mechanism of benzene decomposition and change in char activity

This section discusses the mechanism of benzene decomposition on the char surface and the change in the char's activity along with the C deposition. Firstly, the char has two different types of surfaces, Type I and Type II, which have clearly different characteristics. Type I surface is initially very active toward benzene, but the activity decreases as the C deposit is accumulated, in other words, consumption of micropores [28,33]. The capacity of Type I surface seems to strongly depend on the initial specific surface area and/or pore volume, as seen in Fig. 9. This is clear from comparison of the properties between Char-2 and Char-3 that were prepared from the same parent lignite. Char-3 had initial specific surface area and pore volume greater by *ca.* 9 and 6 times than

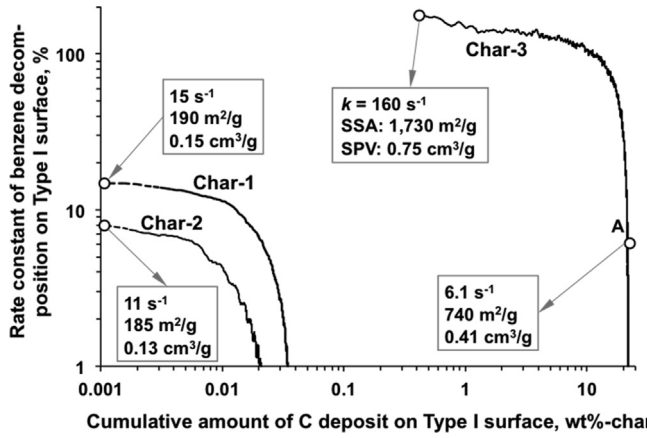

Fig. 9. Changes in the first-order rate constant of benzene decomposition on Type I surface along with C deposition thereon. *k*; first-order rate constant of benzene decomposition on Type I surface, SSA; specific surface area determined by the QS-DFT method, SPV; specific pore volume determined by the QS-DFT method. Point A indicates Char-3 after 30-min exposure to benzene vapor (R4.4).

those of Char-2, respectively, and provided first-order rate constant higher by 15 times. However, it is at present difficult to discuss the change in the surface activity based on the porous properties. As indicated by the point 'A', Char-3 still has a specific surface area and pore volume of 740 m^2/g and 0.41 cm^3/g (42% and 55% of the initials, respectively), where the cumulative amount C deposit has reached *ca.* 99% of the capacity. This indicates that only a part of Type I surface was available for the benzene decomposition. Char-2 has an initial specific pore volume that is about 1/6 of that possessed by Char-3, but the capacity of Char-2 is only 1/170 of the Char-3's capacity.

Fig. 10 shows the pore size distributions of the fresh and spent chars. Exposure of Char-3 to benzene vapor for 30 min decreased the volume of pores with width smaller than 2.0 nm by about a half. However, the remaining pores hardly provided Type I surface. It is estimated that benzene was decomposed forming C deposit filling micropores and also plugging or narrowing their mouths, preventing benzene vapor from diffusing into 'remaining' those pores. The pore width distribution of the spent Char-3 strongly suggests that those pores were finally closed by further exposure to benzene vapor that was decomposed exclusively on Type II surface. The pores with width of 2–3 nm resulted from the C deposition onto Type II surface. The initial pores of Char-1 and Char-2 with width of 1–2 nm would be narrowed and finally closed in the same way as for Char-3 but much more quickly.

Secondly, Type II surface has characteristics clearly different from Type I surface. Its activity, represented by the benzene conversion or its rate constant, is steady regardless of C deposit accumulation. According to the results from the sequential runs with Char-1, the pathways and fate of benzene are drawn in Fig. 11. Benzene chemisorbed onto Type II surface is converted mainly to carbon there and also to diaromatics (mainly biphenyl) and heavier aromatics, which are desorbed from the surface. The heavier aromatics, of which composition is unknown, are further and completely converted to C deposit onto the reactor wall downstream of the char bed. A residence time of benzene vapor as short as 7.6 ms allowed diaromatics and heavier ones to escape from the char bed. A technical subject left for future work is to provide a reactor system that enables to detect and quantify the heavier aromatics minimizing their further conversion into C deposit. From the results shown in Figs. 9 and 10, it is speculated that Type II surface arises from macropores into which benzene vapor easily diffuse, therefore providing stable activity even after deposition of substantial amount of carbon.

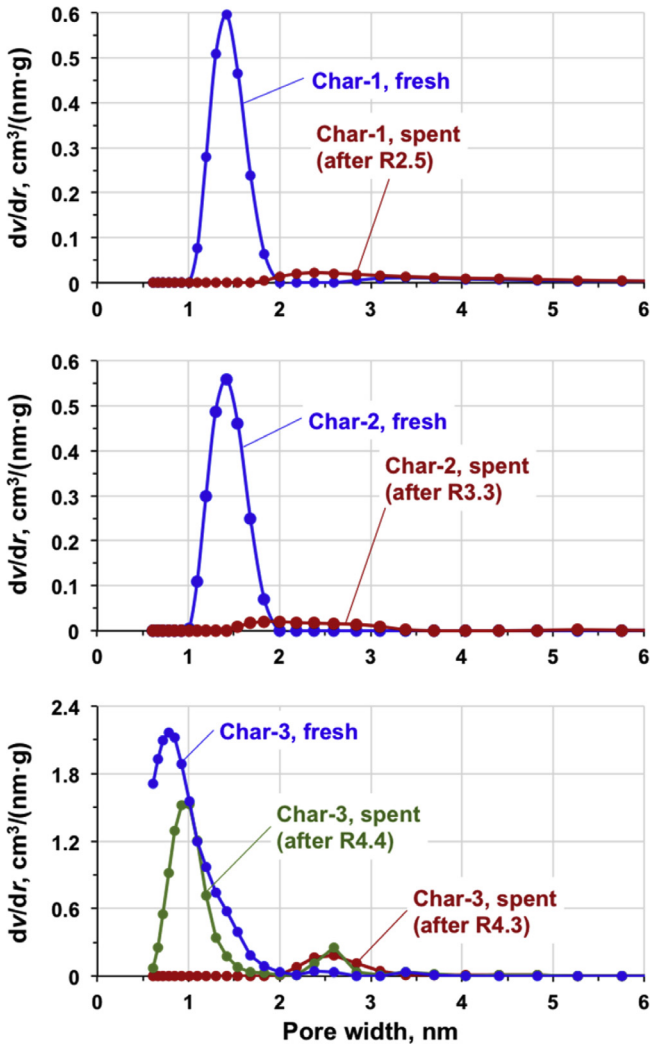

Fig. 10. Pore size distributions for fresh and spent Char-1, Char-2 and Char-3.

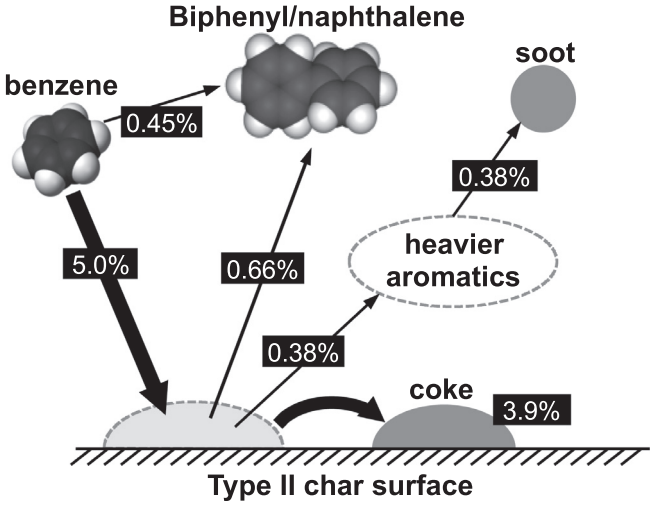

Fig. 11. Pathways of benzene conversion on Type II surface. The indicated conversions are based on the results from R2.1 to R2.5.

4. Conclusions

The authors developed a method to continuously monitor the thermal decomposition of aromatic vapor on the surface of char

particles in a form of micro fixed bed, and revealed the following characteristics of benzene decomposition.

- The char provides two different types of surfaces (Types I and II).
- Type I surface is very active toward benzene vapor, but the activity is consumptive. The activity is lost along with the C deposition. The CO_2 gasification of Char-2 up to its conversion of 60% increases the initial rate constant of benzene conversion into C deposit and capacity to 15 and 170 times, respectively.
- The activity of Type II surface is lower than that of Type I surface, but steady over the time range examined and cumulative amount of C deposit. Benzene undergoes conversion mainly into C deposit but also diaromatics (biphenyl and trace naphthalene) and heavier aromatics, the latter of which escaped the char bed and further converted into C deposit on the reactor wall at downstream.

Acknowledgments

A part of this work was financially supported by New Energy and Industrial Technology Development Organization, Japan, for an R/D project on next-generation coal gasification system. Another part was supported by the Japan Society for the Promotion of Science (JSPS) for Grant-in-Aid for Scientific Research (Grant 17H01340). The authors are grateful to the Cooperative Research Program of Network Joint Research Center for Materials and Devices that has been supported by the Ministry of Education, Culture, Sports, Science and Technology (MEXT), Japan, for material characterization. Cheolyong Choi acknowledges the Kyushu University Program for Leading Graduate Schools: Global Strategy for Green Asia for his financial support.

Appendix A. Supplementary data

Supplementary data to this article can be found online at https://doi.org/10.1016/j.crcon.2018.12.001.

References

[1] L. Devi, K.J. Ptasinski, F.J.J.G. Jansen, A review of the primary measures for tar elimination in biomass gasification processes, Biomass Bioenergy 24 (2003) 125–140.
[2] Z. Abu El-Rub, E.A. Bramer, G. Brem, Review of catalysts for tar elimination in biomass gasification processes, Ind. Eng. Chem. Res. 43 (2004) 6911–6919.
[3] C.-Z. Li, Some recent advances in the understanding of the pyrolysis and gasification behaviour of Victorian brown coal, Fuel 86 (2007) 1664–1683.
[4] J.-I. Hayashi, S. Kudo, H.-S. Kim, K. Norinaga, K. Matsuoka, S. Hosokai, Low-temperature gasification of biomass and lignite: consideration of key thermochemical phenomena, rearrangement of reactions, and reactor configuration, Energy Fuels 28 (2014) 4–21.
[5] S.K. Chembukulam, A.S. Dandge, N.L. Kovllur, R.K. Seshaglri, R. Valdyeswaran, Smokeless fuel from carbonized sawdust, Ind. Eng. Chem. Prod. Res. Dev. 20 (1981) 714–719.
[6] P. Brandt, E. Larsen, U. Henriksen, High tar reduction in a two-stage gasifier, Energy Fuels 14 (2000) 816–819.
[7] J.-I. Hayashi, H. Takahashi, M. Iwatsuki, K. Essaki, A. Tsutsumi, T. Chiba, Rapid conversion of tar and char from pyrolysis of a brown coal by reactions with steam in a drop-tube reactor, Fuel 79 (2000) 439–447.
[8] J.-I. Hayashi, M. Iwatsuki, K. Morishita, A. Tsutsumi, C.-Z. Li, T. Chiba, Roles of inherent metallic species in secondary reactions of tar and char during rapid pyrolysis of brown coals in a drop-tube reactor, Fuel 81 (2002) 1977–1987.
[9] O. Masek, S. Hosokai, K. Norinaga, C.-Z. Li, J.-I. Hayashi, Rapid gasification of nascent char in steam atmosphere during the pyrolysis of na- and ca-ion-exchanged brown coals in a drop-tube reactor, Energy Fuels 23 (2009) 4496–4501.
[10] T. Matsuhara, S. Hosokai, K. Norinaga, K. Matsuoka, C.-Z. Li, J.-I. Hayashi, In-situ reforming of tar from the rapid pyrolysis of a brown coal over char, Energy Fuels 24 (2010) 76–83.
[11] S. Hosokai, K. Kishimoto, K. Norinaga, C.-Z. Li, J.-I. Hayashi, Characteristics of gas-phase partial oxidation of nascent tar from the rapid pyrolysis of cedar sawdust at 700–800 °C, Energy Fuels 24 (2010) 2900–2909.
[12] X. Zeng, Y. Wang, J. Yu, S. Wu, J. Han, S. Xu, G. Xu, Gas upgrading in a downdraft fixed-bed reactor downstream of a fluidized-bed coal pyrolyzer, Energy Fuels 25 (2011) 5242–5249.
[13] T. Sueyasu, T. Oike, A. Mori, S. Kudo, K. Norinaga, J.-I. Hayashi, Simultaneous steam reforming of tar and steam gasification of char from the pyrolysis of potassium-loaded woody biomass, Energy Fuels 26 (2012) 199–208.
[14] K. Matsuoka, S. Hosokai, K. Kuramoto, Y. Suzuki, Enhancement of coal char gasification using a pyrolyzer-gasifier isolated circulating fluidized bed gasification system, Fuel Process. Tech. 109 (2013) 43–48.
[15] L.-X. Zhang, T. Matsuhara, S. Kudo, J.-I. Hayashi, K. Norinaga, Rapid pyrolysis of brown coal in a drop-tube reactor with co-feeding of char as a promoter of in situ tar reforming, Fuel 112 (2013) 681–686.
[16] T. Oike, S. Kudo, H. Yang, J. Tahara, H.-S. Kim, R. Koto, K. Norinaga, J.-I. Hayashi, Sequential pyrolysis and potassium-catalyzed steam-oxygen gasification of woody biomass in a continuous two-stage reactor, Energy Fuels 28 (2014) 6407–6418.
[17] X. Nitsch, J.-M. Commandré, J. Valette, G. Volle, E. Martin, Conversion of phenol-based tars over biomass char under H_2 and H_2O atmospheres, Energy Fuels 28 (2014) 6936–6940.
[18] Y.-L. Zhang, Y.-H. Luo, W.-G. Wu, S.-H. Zhao, Y.-F. Long, Heterogeneous cracking reaction of tar over biomass char, using naphthalene as model biomass tar, Energy Fuels 28 (2014) 3129–3137.
[19] Y.-L. Zhang, W.-G. Wu, S.-H. Zhao, Y.-F. Long, Y.-H. Luo, Experimental study on pyrolysis tar removal over rice straw char and inner pore structure evolution of char, Fuel Process. Tech. 134 (2015) 333–344.
[20] H. Yang, S. Kudo, K. Norinaga, J.-I. Hayashi, Steam-oxygen gasification of potassium-loaded lignite: proof of concept of type IV gasification, Energy Fuels 30 (2016) 1616–1627.
[21] Z.-Y. Du, X. Wang, Y.-H. Qin, Z.-H. Zhang, J. Feng, W.-Y. Li, Effects of secondary reactions on the destruction of cellulose-derived volatiles during biomass/coal co-gasification, Energy Fuels 30 (2016) 1145–1153.
[22] X. Zeng, Y. Dong, F. Wang, P. Xu, R. Shao, P. Dong, G. Xu, L. Dong, Fluidized bed two-stage gasification process for clean fuel gas production from herb residue: fundamentals and demonstration, Energy Fuels 30 (2016) 7277–7283.
[23] D. Feng, Y. Zhao, Y. Zhang, Z. Zhang, H. Che, S. Sun, Experimental comparison of biochar species on in-situ biomass tar H_2O reforming over biochar, Int. J. Hydrog. Energy 42 (2017) 24035–24046.
[24] D. Feng, Y. Zhao, Y. Zhang, S. Sun, Effects of H_2O and CO_2 on the homogeneous conversion and heterogeneous reforming of biomass tar over biochar, Int. J. Hydrog. Energy 42 (2017) 13070–13084.
[25] D. Feng, Y. Zhang, Y. Zhao, S. Sun, J. Gao, Improvement and maintenance of biochar catalytic activity for in-situ biomass tar reforming during pyrolysis and H2O/CO2 gasification, Fuel Process. Tech. 172 (2018) 106–114.
[26] Y. Kawabata, H. Nakagome, T. Wajima, S. Hosokai, H. Sato, K. Matsuoka, Tar emission during pyrolysis of low rank coal in a circulating fluidized bed reactor, Energy Fuels 32 (2018) 1387–1394.
[27] M. Morin, X. Nitsch, M. Hémati, Interactions between char and tar during the steam gasification in a fluidized bed reactor, Fuel 224 (2018) 600–609.
[28] S. Hosokai, K. Kumabe, M. Ohshita, K. Norinaga, C.-Z. Li, J.-I. Hayashi, Mechanism of decomposition of aromatics over charcoal and necessary condition for maintaining its activity, Fuel 87 (2008) 2914–2922.
[29] Z. Abu El-Rub, E.A. Bramer, G. Brem, Experimental comparison of biomass chars with other catalysts for tar reduction, Fuel 87 (2008) 2243–2252.
[30] M. Morgalla, L. Lin, M. Strand, Decomposition of benzene using char aerosol particles dispersed in a high-temperature filter, Energy 118 (2017) 1345–1352.
[31] M. Morgalla, L. Lin, M. Strand, Benzene conversion in a packed bed loaded with biomass char particles, Energy Fuels 32 (2018) 554–560.
[32] L. Burhenne, T. Aicher, Benzene removal over a fixed bed of wood char: The effect of pyrolysis temperature and activation with CO_2 on the char reactivity, Fuel Process. Tech. 127 (2014) 140–148.
[33] F. Nestler, L. Burhenne, M.J. Amtenbrink, T. Aicher, Catalytic decomposition of biomass tars: The impact of wood char surface characteristics on the catalytic performance for naphthalene removal, Fuel Process. Tech. 145 (2016) 31–41.
[34] D. Fuentes-Cano, A. Gómez-Barea, S. Nilsson, P. Ollero, Decomposition kinetics of model tar compounds over chars with different internal structure to model hot tar removal in biomass gasification, Chem. Eng. J. 228 (2013) 1223–1233.
[35] D. Fuentes-Cano, F. Parrillo, G. Ruoppolo, A. Gómez-Barea, U. Arena, The influence of the char internal structure and composition on heterogeneous conversion of naphthalene, Fuel Process. Tech. 172 (2018) 125–132.
[36] S. Hosokai, J.-I. Hayashi, T. Shimada, Y. Kobayashi, K. Kuramoto, C.-Z. Li, T. Chiba, Spontaneous generation of tar decomposition promoter in a biomass steam reformer, Chem. Eng. Res. Des. 83 (A9) (2005) 1093–1102.